



Research article

3D printed trabeculae conditionally reproduce the mechanical properties of the actual trabeculae - A preliminary study

Liqin Zheng^{a,1}, Xiuhong Huang^{b,c,1}, Chihung Li^d, Pengfei Li^{e,f,*}, Ziling Lin^{g,**}, Shaohong Huang^{b,c,***}^a The First Clinical Medical College, Guangzhou University of Chinese Medicine, Guangzhou, China^b Stomatological Hospital, Southern Medical University, Guangzhou, China^c School of Stomatology, Southern Medical University, Guangzhou, China^d International College, Guangzhou University of Chinese Medicine, Guangzhou, China^e Department of Orthopedics, The Affiliated Jiangmen Traditional Chinese Medicine Hospital of Jinan University, Jiangmen, China^f Department of Orthopedics, Jiangmen Central Hospital, Affiliated Jiangmen Hospital of Sun Yat-sen University, Jiangmen, China^g Department of Orthopedics, The First Affiliated Hospital of Guangzhou University of Chinese Medicine, Guangzhou, China

ARTICLE INFO

Keywords:

3D printing
Trabecular bone
Biomechanics
Strain rate
Linear regression

ABSTRACT

Three-dimensional (3D) printing has been used to fabricate synthetic trabeculae models and to test mechanical behavior that cannot be recognized in the actual sample, but the extent to which 3D printed trabeculae replicate the mechanical behavior of the actual trabeculae remains to be quantified. The aim of this study was to evaluate the accuracy of 3D printed trabeculae in reproducing the mechanical properties of the corresponding actual trabeculae. Twelve human trabecular cubes ($5 \times 5 \times 5$ mm) were scanned by micro-CT to form the trabecular 3D model. Each trabecular 3D model was scaled $\times 2$ -, $\times 3$ -, $\times 4$ - and $\times 5$ -fold and then printed twice at a layer thickness of $60 \mu\text{m}$ using poly (lactic acid) (PLA). The actual trabecular cubes and the 3D-printed trabecular cubes were first compressed under a loading rate of 1 mm/min; another replicated stack of 3D-printed trabecular cubes was compressed under a strain rate of 0.2/min. The results showed that the stiffness of the printed cubes tended to increase, while the strength tended to converge when the magnification increased under the two loading conditions. The strain rate effect was found in the printed cubes. The correlation coefficient (R^2) of the mechanical properties between the printed and actual trabeculae can reach up to 0.94, especially under $\times 3$ -, $\times 4$ - and $\times 5$ -fold magnification. In conclusion, 3D printing could be a potential tool to evaluate the mechanical behavior of actual trabecular tissue *in vitro* and may help in the future to predict the risk of fracture and even personalize the treatment evaluation for osteoporosis and other trabecular bone pathologies.

1. Introduction

Osteoporosis is one of the most disabling consequences of aging and is characterized by bone loss and microarchitectural deterioration. Osteoporosis can be treated in a variety of ways, with the fundamental purpose of promoting bone formation and/or inhibiting osteoclast activity to maintain or increase bone mass. It is indispensable to evaluate bone mass pre- and after anti-osteoporosis therapy. Since it has not yet been able to measure bone strength noninvasively, osteoporosis is usually diagnosed by measuring bone mineral density (BMD) using dual-energy X-ray

absorptiometry (DXA) (Keaveny et al., 2020). To date, BMD is still the gold standard for osteoporosis evaluation, fracture risk prediction and drug efficacy assessment (Reid, 2021). However, this approach is still limited in two ways. First, BMD can account for only approximately 70% of bone strength (NCDPO., 2001) and provides no information on trabecular microarchitecture, remodeling rate and so forth (Bouxsein, 2003; Davison et al., 2009; Keaveny et al., 2001). In particular, a fair and even negative correlation between an increase in BMD and a decrease in bone fracture risk has been frequently reported in the literature (Blake et al., 2009; Chen et al., 2022; McNamara, 2010). Second, rates of

* Corresponding author.

** Corresponding author.

*** Corresponding author.

E-mail addresses: lpfdedicated@yeah.net (P. Li), 13600460045@sina.cn (Z. Lin), hsh.china@tom.com (S. Huang).¹ These authors contributed equally.

diagnostic testing by DXA are low. Only 9.5% of eligible Medicare women and 1.7% of men are diagnostically screened for osteoporosis by DXA (Zhang et al., 2012). The low screening rate is concerning because it impedes anti-osteoporosis treatment and is thought to be responsible for the increasing incidence of hip fractures in the USA (Lewiecki et al., 2018). Given these limitations, there is a critical need to develop alternative tools to improve bone strength evaluation and fracture risk prediction.

With advances in stereology, it is more convenient to obtain the three-dimensional (3D) morphology of trabecular bone (Bouxsein et al., 2010). The bone volume fraction (BV/TV) and fabric anisotropy (DA) derived from the 3D images (hundreds even thousands of two dimensional binary images were stacked slice by slice to be three dimensional, the BV/TV and DA are calculated based on 3D images) are supposed to be the most direct measures of bone mass and bone loss. BV/TV alone explained 87% of the trabecular elastic properties, while DA plus further described 10%, and the improvement in variance explained by adding other independent factors (e.g., trabecular number, thickness, separation, etc.) was marginal (<1%) (Maquer et al., 2015). In addition, the tissue properties (e.g., mineralization, collagen matrix, etc.) was proven to have a slight influence on the elastic property of trabecular bone (Liu et al., 2019). It could be said that trabecular volume and microarchitecture are the determinants of trabecular mechanical properties. If one can noninvasively replicate the trabecular volume and microarchitecture from a living body, then the biomechanical properties of trabeculae under varied conditions (e.g., bone remodeling, osteoporosis diagnosis and treatment efficacy of anti-osteoporosis) could be *in vitro* three-dimensionally quantified.

The finite element method (FEM) is an *in vitro* solution that is used to predict the mechanical behavior of trabeculae and look inside the microstructure to find where stresses are concentrated and may cause fracture (Alomari et al., 2018; Hambli, 2013; Liu et al., 2012; Silva et al., 1998). FEM is a computer-based simulation that predicts how an object will respond to a specific assigned loading in the real world. The FEM model is a component of discrete elements, and its mechanical behavior is described by a mathematical equation. However, every FEM simulation on bone structure must assume mechanical parameters such as elastic modulus and Poisson's ratio in advance and finally be validated with *in vitro* mechanical testing to confirm that accurate mechanical properties are predicted (Ni et al., 2016; Uppuganti et al., 2022; Zhou et al., 2016). One can conduct the confirmation on cadaveric samples but barely on a living body because of the medical ethics. Furthermore, a finite element simulation usually results in massive models with millions of elements and nodes, which requires a strong computer. In addition, the output can only be as good as the input since FEM demonstrates a steep learning curve.

3D printing provides an alternative tool to three-dimensionally quantify the biomechanical properties of trabeculae *in vitro*. 3D printing is a process that enables the build of 3D shapes from computer aided design (CAD) representations by incremental deposition of printing material (Büşra and Şeyma, 2022; Mohammad Reza et al., 2020). 3D printing can allow two-dimensional images developed from micro-CT scans to be transferred directly to STL files for replicating the trabecular structure with high precision and accuracy (Barak and Black, 2018). Furthermore, 3D printing provides an opportunity to repeatedly test the trabecular sample under varied loading and structural conditions that cannot be conducted on actual trabecular bone (Amini et al., 2020; Dobson et al., 2006; Kuhn et al., 2014b; Langton et al., 1997; Tellis et al., 2008; Wood et al., 2019; Yoon et al., 2014). However, to our knowledge, previous studies that attempted to mechanically test 3D-printed trabecular bone did not correlate their results to the corresponding actual bone, and the extent to which 3D-printed trabeculae replicate the mechanical behavior of actual trabeculae remains to be quantified.

In this study, we attempt to introduce and validate 3D printing as a useful alternative tool to assess trabecular mechanical properties with the aim of noninvasively improving bone strength evaluation. To this end, a

series of mechanical tests on 3D printed trabeculae and the corresponding actual trabeculae was conducted to quantify the relation using a specified printing material. Specifically, we attempt to ① define the efficiency of BV/TV in explaining the variance of elastic properties in 3D-printed trabeculae; ② determine how magnification of 3D-printed trabecular samples under different loading rates and strain rates affects their properties contents; and ③ correlate mechanical properties between the actual trabecular bone samples and their 3D-printed replicas. Our preliminary study provides potential options to estimate the mechanical properties of trabecular tissue using 3D printing to improve osteoporosis diagnosis accuracy.

2. Methods

An overview of the study is presented in Figure 1.

2.1. Sample preparation and micro-CT scanning

An 83-year-old male who underwent left hip hemiarthroplasty because of femoral neck fracture induced by a sideways fall was recruited. Ethical committee approval was obtained, and the patient was informed and signed a consent form before the procedure. The femoral head was collected after the surgery and stored at -80 °C prior to trabecular cube segmentation. After being unfrozen and fixed with 4% paraformaldehyde for 48 h, 12 volume of interest (VOI) cubes (5 × 5 × 5 mm) were randomly segmented from the domain of the femoral head. Figure 2(a). The opposite sides of the cubes were cut during the same machining operation to ensure parallelism and minimize geometric imperfections. This operation was performed with an EXAKT precision cutting and grinding system. The cutting speeds were adjusted to minimize trabecular network damage (heating or shearing of the samples). The VOI cubes were then scanned by a micro-CT scanner (SkyScan 1276, Bruker, USA) at 20 µm resolution with a voltage of 100 kV and current of 200 µA Figure 2(b). In CTAn 1.16.8 (SkyScan, Bruker, USA) software, the global threshold of 45–255 was chosen to reconstruct VOI cubes and to acquire the BV/TV value. VOI cubes were saved in “stl” format for 3D printing. Figure 2(c).

2.2. 3D printing

Each VOI cube was scaled ×2-, ×3-, ×4- and ×5-fold by Materialise Magics 21.0 (Materialise, Belgium) prior to 3D printing. VOI cubes were printed by an HP Jet Fusion 3D printer (Hewlett-Packard, USA) using poly (lactic acid) (PLA) at a layer thickness of 60 µm, which is smaller than the dimensions of the magnified cubes. After 3D printing but prior to mechanical testing, the support material (base and bar) within the cubes was carefully manually removed according to the manufacturer's instructions. Figure 2(d). The printed cubes were mechanically tested as soon as possible after the printing process, since PLA is degradable in an *in vitro* environment, although the degradation is very slow (Promnil et al., 2022). There was a one-day gap between the printing of the cubes and the beginning of the support material removal process and a half-day gap between the support material removal process and mechanical testing.

It is necessary to magnify the VOI cubes because the actual trabeculae are quite minute-sized, which may exceed the printing ability of some printers and cause failed printing. For example, at the beginning, we attempted to print the trabecular cubes at the original size but end up with failure because a layer thickness of 60 µm does exceed the actual dimension of some trabeculae; however, it turns to success after the magnification process. Furthermore, we aim to investigate the effect of magnification on mechanical properties in the hope of providing an application suggestion in the future.

The HP Jet Fusion 3D printer was applied since the machine uses a technique called Multi-Jet Fusion, which offers low machining time, high part properties and minimal post production finishing compared to

existing 3D printing technologies. Briefly, the 3D printing process is as follows: First, the build material is recoated on the surface layer. The printing process applies a fusing agent selectively to the places where the 3D object to be and applies a detailing agent where the fusing action needs to be controlled. Radiation energy is applied on the entire surface so that the area for the 3D object is fused. This process is repeated layer by layer until the full 3D object is printed (Hokeun Kim et al., 2016; Singh and Pervaiz, 2021).

PLA has been widely used to reproduce skeletal mechanical properties because PLA has elastic behavior similar to that of trabecular bone and has advantages in biocompatibility and biodegradability (Baptista and Guedes, 2021; Senatov et al., 2016; Wu et al., 2020). It should be mentioned that we could have printed the trabecular cubes at a thinner layer (e.g., $\sim 20 \mu\text{m}$), but PLA cannot support such a high accuracy because PLA only works at layer thicknesses $\geq 50 \mu\text{m}$ using our printer. In addition, we could have adopted other polymers, such as acrylonitrile butadiene styrene (ABS), as filaments (Yoon et al., 2014), yet their elastic modulus and strength are quite different from those of bone tissue according to our experience. Other polymer printing resins may also demonstrate a tension-compression strength asymmetry that is similar to bone material but cannot be a candidate in bone tissue engineering (Barak and Black, 2018; Wood et al., 2019).

The printing accuracy could be conducted by correlating the weight of the printed cubes with their volume fraction (Barak and Black, 2018; Wood et al., 2019) or using micro-CT scanning and the FEM model to validate printing accuracy and precision (Dobson et al., 2006; Grzeszczak et al., 2021; Kuhn et al., 2014b; Tellis et al., 2008), but these approaches only reveal the accuracy of structure replicability rather than the mechanical behavior. In this study, we did not verify the structure replicability since we focused on replicating the accuracy of the macromechanical behavior.

2.3. Mechanical testing

The printed cubes were loaded in a direction that was perpendicular to the printing layers because under the alignment, the 3D-printed trabecular bone will respond with optimal mechanical behavior (Doktor et al., 2018). The actual trabecular cubes and the corresponding printed cubes were kept under an alignment that loaded onto the same plane. Both actual trabecular cubes and 3D printed cubes were loaded in uniaxial compression testing using a universal testing machine (Jingzhuo

Machinery Factory, Yangzhou, China) equipped with a 10 kN load cell with an error of 0.3% of the indication value. First, the actual trabecular cubes and the 3D printed cubes were compressed at a loading rate of 1 mm/min. For the actual trabecular cube, a loading rate of 1 mm/min equal to a strain rate of 0.2/min, and for $\times 2$, $\times 3$, $\times 4$ and $\times 5$ printed cubes equal to 0.1/min, 0.067/min, 0.05/min and 0.04/min, respectively. Second, another stack of 3D printed cubes was loaded at a strain of 0.2/min. To reduce shear stress due to friction between loading surfaces and samples, we used low-friction polished stainless steel anvils and applied a small preload of 5 N to 'tighten' the load cell-anvil interface before the experiment started (Wood et al., 2019). Only then load and deformation data were started to be collected. The measurements were recorded at 25 Hz (every 40 ms).

2.4. Data analysis and statistics

The stiffness was defined as the slope of the load–displacement curve in the linear stage (Figure 3(a)). The measured load was normalized by dividing the cross-sectional area to derive the stress, and the strength was defined as the maximal stress value (Figure 3(b)).

One-way ANOVA (SPSS 20.0, IBM, USA) was performed to identify significant differences in stiffness and strength among groups. A least squares regression function was used to determine the coefficients of a linear function in the form (Jin et al., 2020):

$Y = Ax + B$, where A and B are coefficients, Y is one of two observed dependent variables (i.e., the stiffness and strength of actual trabecular cubes) estimated as a function of the printed stiffness and strength (x) (Barak and Black, 2018). We also used the formulas to describe the correlation between the printed mechanical properties and BV/TV. The correlation coefficient R^2 is included. A P value < 0.05 was considered to be statistically significant.

3. Results

3.1. Average stiffness and strength

The stiffness of the printed cubes increases significantly (Figure 4(a)), while the strength shows a less significant increase with increasing magnification (Figure 4(b)). Under a loading rate of 1 mm/min, the printed cubes from $\times 2$ to $\times 5$ magnification show average stiffnesses of 131.26, 309.02, 462.89 and 588.70 N/mm; average strengths of 1.06,

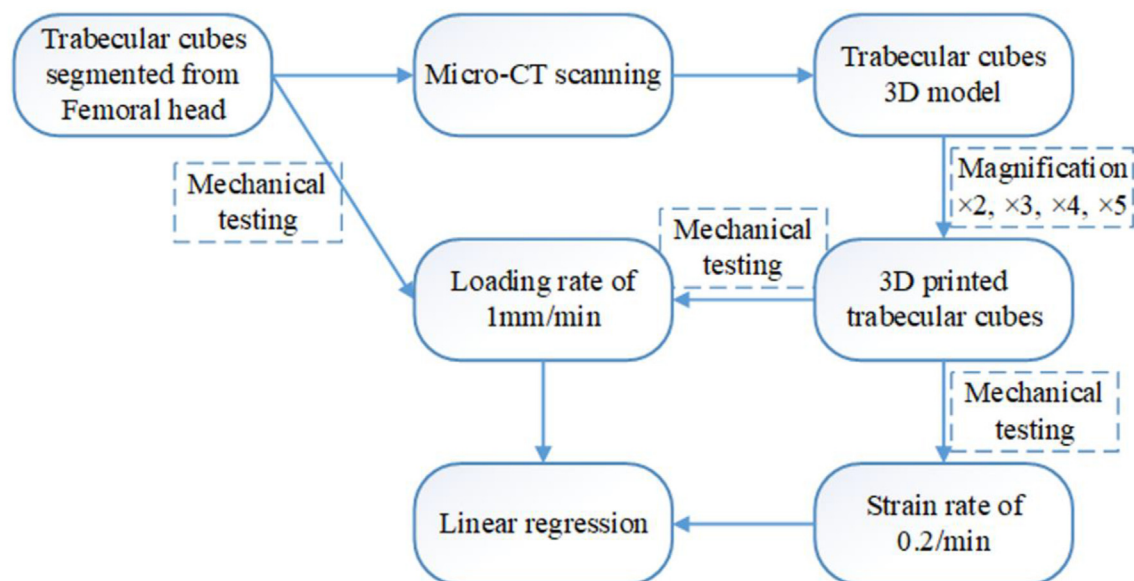


Figure 1. Overview of this study.

1.61, 1.87 and 1.79 MPa, respectively. Under a strain rate of 0.2/min, the printed cubes from $\times 2$ to $\times 5$ magnification display average stiffnesses of 235.58, 347.17, 531.05 and 668.75 N/mm; average strengths of 1.94, 2.09, 2.23 and 2.15 MPa, respectively. The actual trabecular cubes exhibit an average stiffness of 255.20 N/mm and strength of 3.34 MPa under a loading rate of 1 mm/min (strain rate of 0.2/min).

The actual trabecular cubes demonstrate a significant difference in stiffness only to $\times 5$ printed cubes under two compression conditions ($P < 0.05$), and the actual trabecular cubes share the most similar average stiffness with $\times 2$ printed cubes (under a strain rate of 0.2/min) and $\times 3$ printed cubes (under a loading rate of 1 mm/min) compared to the other magnifications. There were no significant differences in strength among each printed group under the same compression conditions ($P > 0.05$), while the actual trabecular cubes showed significant differences in each printed group ($P < 0.05$). The strength of the actual trabecular cubes was approximately 3.15, 2.07, 1.79, and 1.87 times that of $\times 2$, $\times 3$, $\times 4$, and $\times 5$ printed cubes under a loading rate of 1 mm/min and was approximately 1.72, 1.60, 1.50, and 1.55 times that under a strain rate of 0.2/min.

3.2. Correlation between BV/TV and printed stiffness

BV/TV is one of the determinants of the variance in the elastic property of trabecular bone, and BV/TV also accounted for the major variance in the stiffness of the printed cubes in our study. However, the explanation efficiency seems higher in the $\times 3$, $\times 4$ and $\times 5$ groups than in the $\times 2$ group, especially in the $\times 5$ group. Nearly each printed cube under a strain rate of 0.2/min demonstrates a higher stiffness and therefore forms a steeper slope of the regression curve Figure 5(a-d).

3.3. Linear regression in stiffness and strength

The stiffness of the printed cubes significantly correlates with the actual trabecular cubes under two compression tests, especially at $\times 3$, $\times 4$ and $\times 5$ magnification. Under a loading rate of 1 mm/min, the stiffness of the actual trabecular cubes can be expressed as a function of $\times 2$, $\times 3$, $\times 4$ and $\times 5$ printed cubes in linear form with coefficients $R^2 = 0.87$, $R^2 = 0.92$, $R^2 = 0.92$ and $R^2 = 0.93$, respectively. Under a strain rate of 0.2/min, the stiffness of the actual trabecular cubes can be determined as a function of $\times 2$, $\times 3$, $\times 4$ and $\times 5$ printed cubes in linear form with coefficients $R^2 = 0.90$, $R^2 = 0.94$, $R^2 = 0.91$ and $R^2 = 0.93$, respectively Figure 6(a-d).

Similarly, the strength of the printed trabecular cubes significantly correlated with the actual trabecular cubes under the two compression conditions. Upon a loading rate of 1 mm/min, the strength of the actual trabecular cubes can be defined as a function of $\times 2$, $\times 3$, $\times 4$ and $\times 5$ printed cubes in linear form with coefficients $R^2 = 0.89$, $R^2 = 0.94$, $R^2 = 0.94$ and $R^2 = 0.94$, respectively. Upon a strain rate of 0.2/min, the strength of the actual trabecular cubes can be described as a function of $\times 2$, $\times 3$, $\times 4$ and $\times 5$ printed cubes in linear form with coefficients $R^2 = 0.93$, $R^2 = 0.92$, $R^2 = 0.91$ and $R^2 = 0.93$, respectively Figure 7(a-d).

4. Discussion

The aim of this study was to quantify the replication accuracy of mechanical properties between the printed trabecular cubes and the actual trabecular cubes using a specified printing material (PLA) at a restricted layer thickness of 60 μm . The evaluated parameters were stiffness and strength based on a series of cube magnifications. We

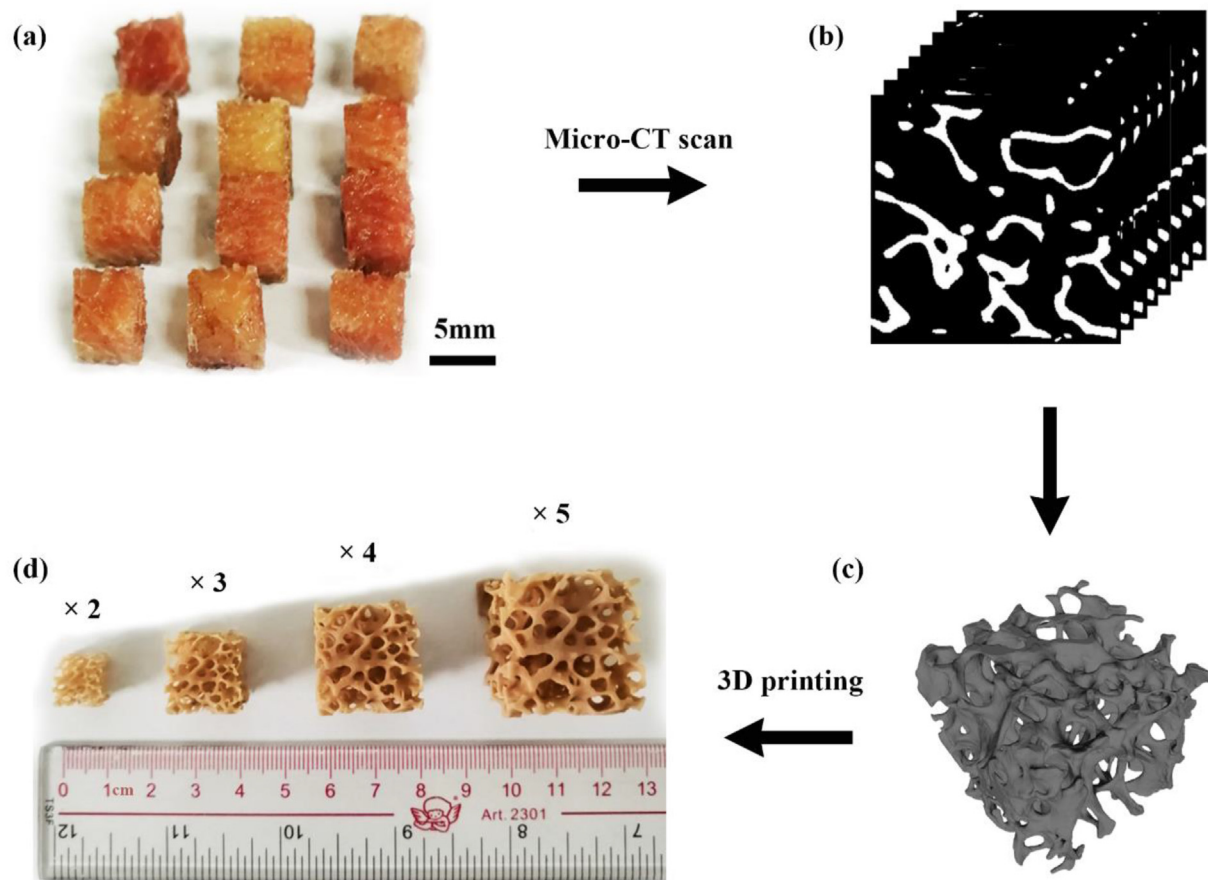


Figure 2. An overview of the main experimental steps as described in the text. (a) Twelve trabecular cubes segmented from the femoral head. (b) Several 2D slices in the transverse plane, displaying the internal trabecular structure. (c) 3D trabecular cube model in “stl” format. (d) Each cube was printed at $\times 2$, $\times 3$, $\times 4$ and $\times 5$ magnification.

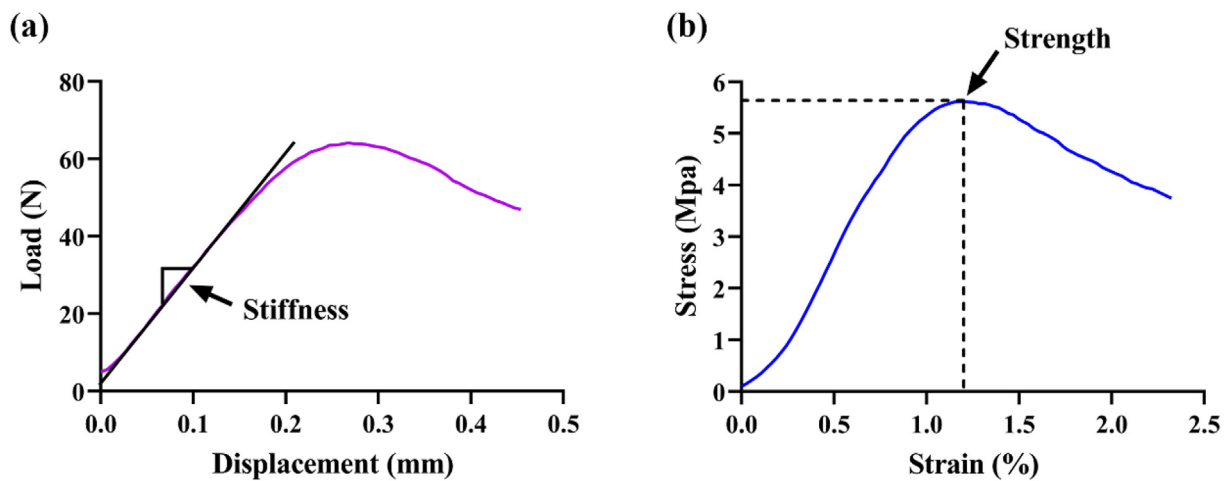


Figure 3. Mechanical properties definition (taking one of the actual trabecular cube curves as an example). (a) The stiffness was defined as the slope of the load–displacement curve; (b) the strength was defined as the maximal stress value of the stress–strain curve.

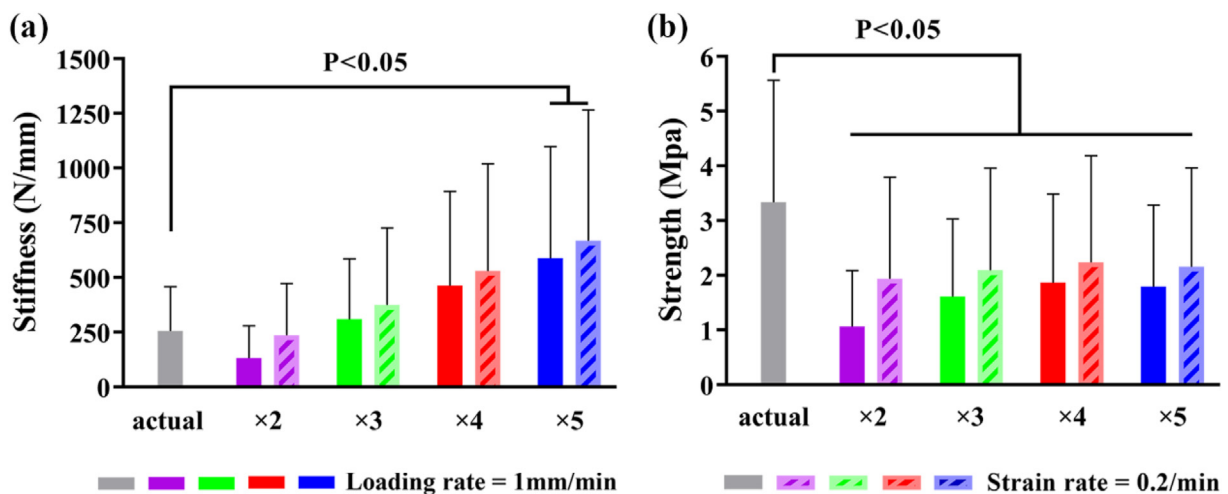


Figure 4. Mechanical test results of each printed group. (a) Stiffness under a loading rate of 1 mm/min and a strain rate of 0.2/min. (b) Strength under a loading rate of 1 mm/min and under a strain rate of 0.2/min. The loading rate of 1 mm/min is represented by a solid bar; the strain rate of 0.2/min is represented by a dashed bar.

confirmed that the known volume fraction–elastic property relation within trabecular tissue also fit the printed trabeculae. We also determined the effect of cube magnification, loading rate and strain rate on the mechanical properties. The observed mechanical variations for the actual trabecular samples were significantly expressed by the corresponding printed trabecular samples under specific magnification. This provides insight into possible applications that will enable us to estimate the biomechanical properties of trabecular tissue *in vitro* using 3D printing in the future.

Different storage methods may cause a change in the properties of bone tissue during mechanical testing. A study demonstrated that paraformaldehyde solution does not influence the biomechanical properties of bone even over a two-week period (Tiefenboeck et al., 2019). Furthermore, no differences in mechanical properties were observed up to 12 and 24 months of cryopreservation at -80°C (Matter et al., 2001; Tiefenboeck et al., 2020). In our study, the femoral head was harvested and stored at -80°C immediately after femoral head extraction, which is one of the main procedures of hemiarthroplasty. Before trabecular cube segmentation, the femoral head was kept at -80°C for one week. We then fixed the trabecular cubes with 4% paraformaldehyde solution for 48 h to maintain the mechanical properties as much as possible, since it took several days to scan and mechanically test the cubes. Theoretically, the process we handled did not change the trabecular mechanical properties.

Another possible point of concern is the sample size and source. Bone tissue is of high anisotropy among populations even within individuals at the same anatomic site of the same bone (Morgan et al., 2018). The mechanical properties may depend on bone mass, microstructure and organic ingredients (Liu et al., 2019). However, the bone mass and microstructure (i.e., BV/TV and DA) are the best determinants of trabecular bone elastic properties as aforementioned; besides, the printed cubes were all printed using the PLA filament, the content of “organic ingredients” was consistent and their influence shall be ignored. Furthermore, in the present study, the actual trabecular BV/TV value ranged between 9% and 31%, which overlapped with a previous study (11%–33%) testing trabecular bone samples from human femoral heads harvested from osteoporotic individuals (Li and Aspden, 1997). A large standard deviation was found in the property results because trabecular tissue within the femoral head has an anisotropic and functionalized distribution. A portion of the high-density area would be segmented out upon random sampling, which would lead to a large standard deviation. In fact, this anatomical variation has been found in most previous studies (Li and Aspden, 1997; Morgan et al., 2003; Tassani et al., 2011; Zhang et al., 2010). Given such preconditions, the variation in population characteristics appears less important. Therefore, we recruited only one patient and segmented the trabecular cubes to obtain the structural features.

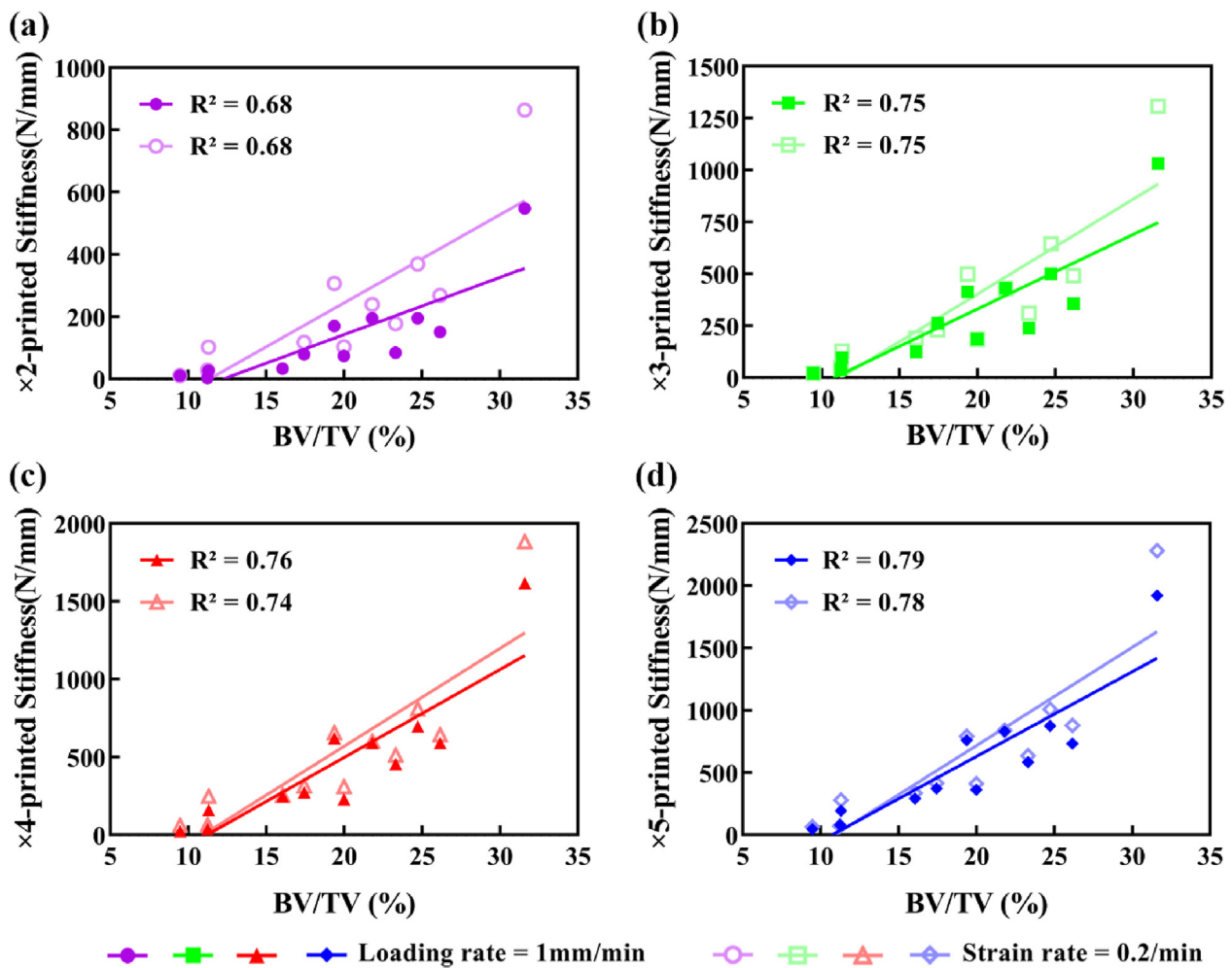


Figure 5. Linear regression between BV/TV and the stiffness of the printed cube under two compression conditions. (a) Coefficient of linear regression between BV/TV and $\times 2$ -printed cubes. (b) Coefficient of linear regression between BV/TV and $\times 3$ -printed cubes. (c) Coefficient of linear regression between BV/TV and $\times 4$ -printed cubes. (d) Coefficient of linear regression between BV/TV and $\times 5$ -printed cubes.

The stiffness of the printed cubes increased significantly with increasing magnification since it was defined as the slope of the load–displacement curve, and the displacement was controlled at a consistent rate for each cube. It costs a larger load to deform a larger cube. However, the strength did not apparently change since it was defined as the maximum stress divided by the cross-sectional area. Using 3D-printed trabecular cubes, investigators reported that an approximately 8% decrease in BV/TV leads to a 24% decrease in structural strength and 17% in structural stiffness (Barak and Black, 2018). By verifying their findings to cadaveric mechanical testing and FEM modeling in publications, they claimed 3D printed trabecular model could be a useful tool to investigate the effect of individual trabecular bone loss on the tissue's mechanical properties. However, the shortcoming of the verification is clear: they did not verify the printing results to the corresponding actual trabecular bone but to allogeneic bone. In this study, we conducted a matched pair experiment between 3D printed trabeculae and the corresponding actual trabeculae to evaluate the relation.

Using stereolithography (compared to Multi-Jet Fusion in our printer), this study investigated the influence of scale factor on trabecular structure replicability and found an optimal scale factor of 1.8 or 2 by comparing the volume difference and trabecular thickness. A higher scale factor did not seem to improve the structure replicability (Grzeszczak et al., 2021). These results are contrary to our results. In the present study, as the magnification increased, the strength of the printed cubes tended to converge at 1.8 MPa upon loading rate of 1 mm/min and tend

to converge at 2.1 MPa upon a strain rate of 0.2/min. These results suggest that magnification would be an appropriate process for attempting to acquire an intact trabecular model. In addition, the BV/TV in determining the printed stiffness of the $\times 2$ group, the printed stiffness and the printed strength of the $\times 2$ group in determining the actual bone were all inferior to those of the other groups, indicating that $\times 2$ magnification was too small to completely replicate the anatomic features of the actual trabeculae and therefore to reproduce the mechanical properties. This may, first, be because part of the tiny trabeculae smaller than 30 μm cannot be printed at a layer thickness of 60 μm even after a 2-fold magnification. Second, the manual postproduction process (removal of the supporting base and bar within the printed cube) may have potentially destroyed some tiny trabeculae within $\times 2$ cubes.

Compared to a consistent strain rate of 0.2/min applied to the printed trabecular cube, a loading rate of 1 mm/min on the printed cubes was equal to strain rates of 0.1/min, 0.067/min, 0.05/min and 0.04/min in the $\times 2$, $\times 3$, $\times 4$ and $\times 5$ groups, respectively. A “strengthen” effect (strain rate effect) was found in the printed trabecular cubes, in which a higher strain rate led to a higher stiffness and strength, which has been recognized in bone tissue (Carter and Hayes, 1977; Linde et al., 1991; Maruyama et al., 2014; Ouyang et al., 1997; Pilcher et al., 2010; Uniyal et al., 2022). The exact cause of the strain rate effect is not clear but could be due to the inherent viscoelasticity of PLA (Nofar et al., 2019). Another potential cause is the delayed buckling of printed trabeculae under high-speed loading. The delayed buckling could be hypothesized as

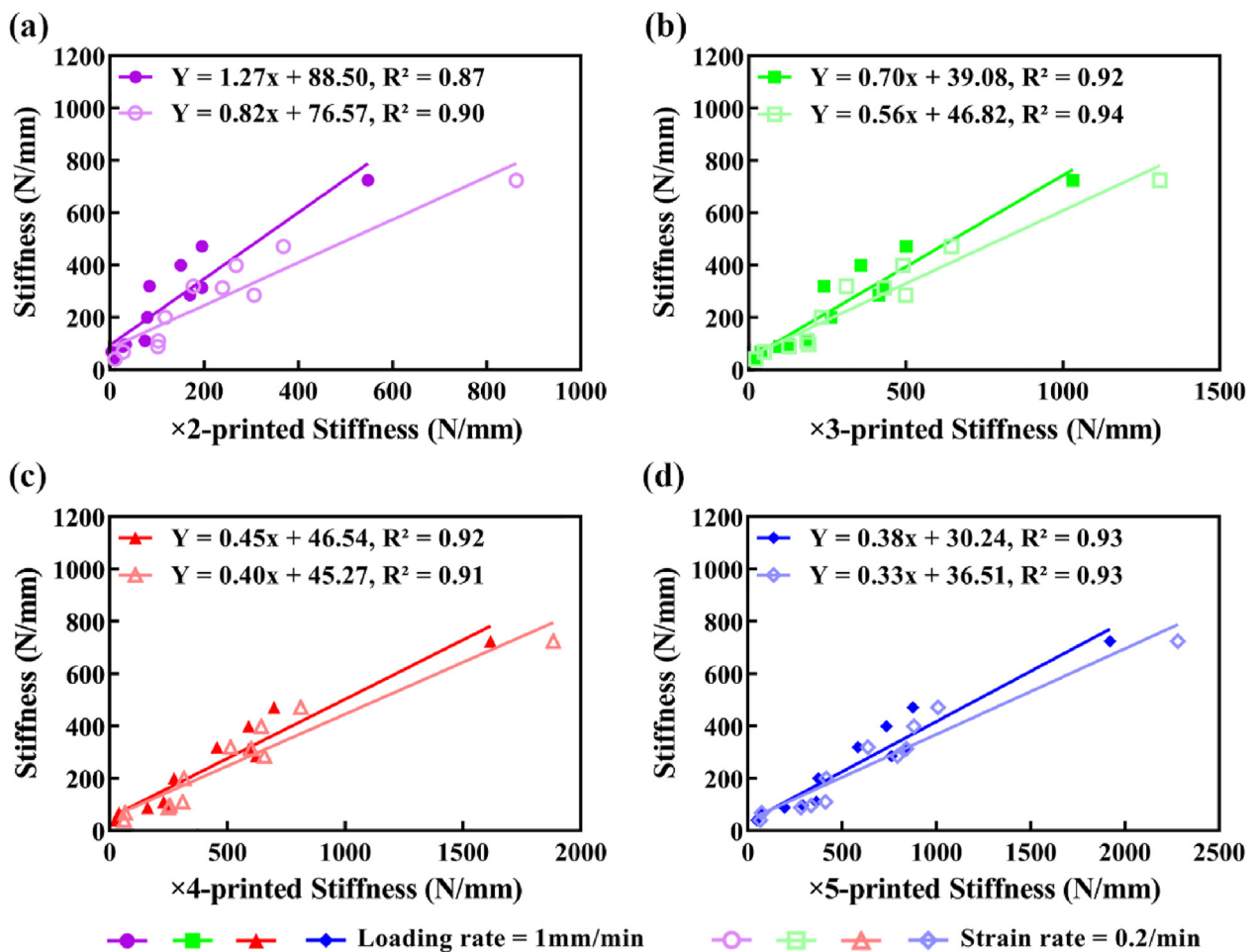


Figure 6. Linear regression between the stiffness of the printed trabecular cubes and the actual trabecular cubes under two compression conditions. (a) Linear regression between $\times 2$ -printed cubes and the actual cubes. (b) Linear regression between $\times 3$ -printed cubes and the actual cubes. (c) Linear regression between $\times 4$ -printed cubes and the actual cubes. (d) Linear regression between $\times 5$ -printed cubes and the actual cubes.

follows: the load increases quite rapidly in a short period of time; even though the buckling load for trabeculae may be exceeded, there is not enough time for the trabeculae to buckle and collapse, as it does in the low strain tests. The load increases rapidly to a level where a different failure mode ensues, which occurs at low strain and high stress (Pilcher et al., 2010).

Significantly linear regression was found in the printed trabecular cubes and the actual trabecular cubes both in stiffness and strength, especially in the $\times 3$, $\times 4$ and $\times 5$ groups. The linear regression accuracy may potentially be affected by marrow pressurization. A previous study showed that although deformation patterns did not differ significantly, trabecular bone showed a decrease in mechanical properties when the marrow was unconfined and allowed flow during compression in the sample (Halgrin et al., 2012). This unexpected decrease was also found in the replicated trabecular bone model using 3D printing under confined conditions where trabecular samples were wrapped to prevent the marrow from flowing out of the sample under loading (Yoon et al., 2014). This is because the marrow induces transverse pressure and extra local stress on trabeculae during its flow, causing the premature collapse of the trabecular network (Halgrin et al., 2012). Trabecular cubes in our study were fixed with paraformaldehyde solution, which led to the condition that marrow became stiffer (i.e., denaturation) than the fresh bone and might account for part of the regression error. Since marrow fills in the trabecular tissue in a living body while a printed trabecular sample is free from marrow wrapping, extra experimental investigation is necessary to acquire the optimal printing condition under varied loading rates (or strain rates).

To our knowledge, only a few previous studies have attempted to investigate the application of 3D printing to replicate and mechanically test replicas of trabecular bone; however, none of them revealed reproducing accuracy from the corresponding real bone samples with respect to mechanical properties. Dobson (Dobson et al., 2006) 3D printed trabecular models based on micro-CT scanning from human iliac crest, femoral head, calcaneus and lumbar vertebrae. They also developed FE models for verification. The compressive stiffness of 3D-printed trabecular models was found to strongly correlate with those predicted by the FE models. They concluded that 3D printing is an important complement for FE analysis to evaluate the mechanical properties of trabecular structures that do not physically exist. In our latest study (Zheng et al., 2022), we also combined 3D printing and FE models to prove that the medial tibial plateau sustains higher physiological stress than the lateral plateau. This result helps explain why varus knee deformities account for the majority of patients with knee osteoarthritis (KOA) and affect more than 70% of patients with idiopathic KOA, as well as the “nonuniform settlement” phenomenon of the medial tibial plateau. Tellis (Tellis et al., 2008) 3D printed the trabecular models of canine femurs and scanned the models using micro-CT. They claimed that the 3D printed trabecular models matched the actual trabecular samples in porosity but not in connectivity density and trabecular separation. These differences were attributed to the low resolution of the 3D printer (250 μm , approximately 5 times lower than that of our 3D printer). However, another study reported high conformity between the actual and reproduced structures using a higher resolution 3D printer. However, they did not mechanically test their samples to determine whether their stiffness and strength

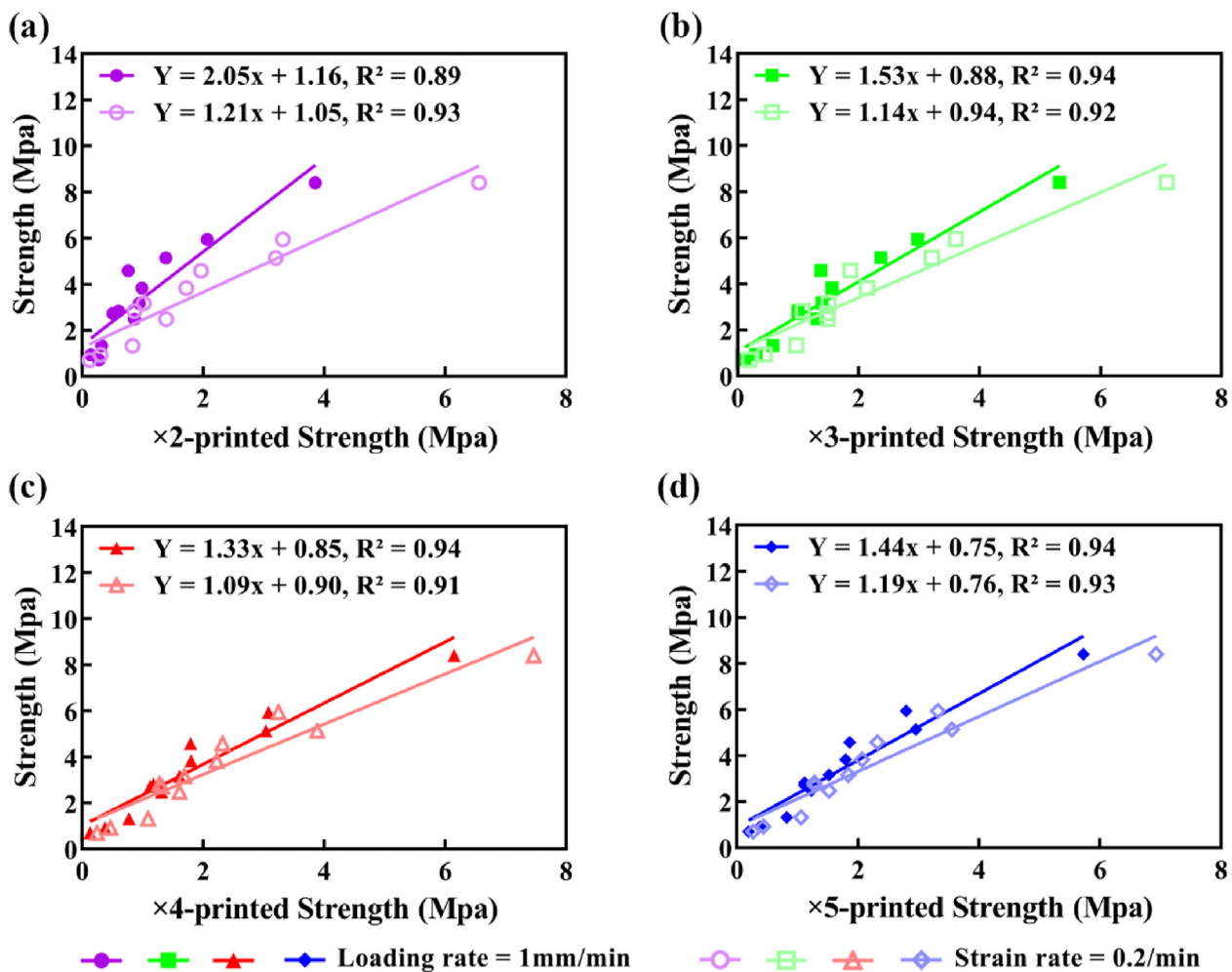


Figure 7. Linear regression between the strength of the printed cube and the actual cube under two compression conditions. (a) Linear regression between $\times 2$ -printed cubes and the actual cubes. (b) Linear regression between $\times 3$ -printed cubes and the actual cubes. (c) Linear regression between $\times 4$ -printed cubes and the actual cubes. (d) Linear regression between $\times 5$ -printed cubes and the actual cubes.

correlated to the actual trabecular bone samples (Kuhn et al., 2014a). Barak and Black (2018) 3D printed series trabecular cubes to compare a healthy 3D printed trabecular bone model with the same model after bone resorption was simulated. They found that under an 8% decrease in BV/TV, the trabecular strength decreased from 9.14 ± 2.85 MPa to 6.97 ± 2.44 MPa, and the stiffness decreased from 282.5 ± 63.4 N/mm to 233.8 ± 51.2 N/mm. They concluded that 3D printing is novel and valuable for quantifying the effect of structural deterioration on the mechanical properties of trabecular bone. Recently, Wood (Wood et al., 2019) 3D printed a trabecular structure and loaded it in compression; they unexpectedly found that a trabecular structure loaded off-mechanical axis tended to have higher stiffness and strength when compared to the same trabecular structure loaded on-mechanical axis, which contradicts Wolff's law. These unexpected results imply that trabecular bone adaptation may serve additional purposes than simply optimizing bone structure to one principal loading scenario.

5. Limitations

First, our study included only one bone sample. Substantial bone samples across wide ages, gender, anatomic site and pathological state should be further verified to prove the universality. Second, 3D printing filaments (PLAs) are isotropic, while bone is hierarchical and anisotropic (e.g., collagen fibers and hydroxyapatite crystal axes are aligned in specific orientations). This has the potential to reduce the biological significance of our results. However, the anisotropic and inhomogeneous

properties of the bone material have a negligible and insignificant effect on the apparent elastic properties (Kabel et al., 1999; Liu et al., 2019). Although the 3D printing filament is mechanically isotropic, a printed model may potentially exhibit anisotropy due to the inherently layer-by-layer construction. However, this possible caveat should not affect our results since all of our printed samples were tested orthogonally to the direction of printing (Barak and Black, 2018). Third, we only used PLA to replicate bone structure. In fact, there are kinds of available commercial printing filaments, and the 3D printing mode can be the candidate (Awad et al., 2021). Their predicted effectiveness should be compared to ours. Last but not least, the process of the micro CT scanning slices (for example, the global threshold setting) indeed influences the integrity of the trabecular structure and the resultant mechanical properties. One should carefully choose the global threshold to maintain the trabecular structure as much as possible.

6. Conclusions

This preliminary study aimed to evaluate the accuracy of 3D-printed trabeculae in reproducing the mechanical behavior of the corresponding actual trabeculae. Our results show that the stiffness of the printed cubes tends to increase, while the strength tends to converge with increasing magnification. The strain rate effect was also recognized in the printed trabecular cubes. The printed mechanical properties significantly correlate with the actual trabecular properties, especially at $\times 3$ -, $\times 4$ - and $\times 5$ -fold magnification. Based on the results obtained, it can be concluded

that 3D printed trabeculae can be used to conditionally predict the mechanical properties of the actual trabeculae. 3D-printed trabeculae provide a potential approach to assess osteoporosis, predict the risk of fragility fracture, and even personalize the treatment evaluation for osteoporosis and other trabecular bone pathologies.

Declarations

Author contribution statement

Liqin Zheng: Conceived and designed the experiments; Performed the experiments; Analyzed and interpreted the data; Wrote and revised the paper.

Xiuhong Huang: Analyzed and interpreted the data.

Chihung Li: Performed the experiments.

Pengfei Li, Ziling Lin and Shaohong Huang: Conceived and designed the experiments; Wrote the paper.

Funding statement

Prof. Ziling Lin was supported by National Natural Science Foundation of China [81673996], National Famous Old Chinese Medicine Expert Inheritance Studio Construction Project [2022].

Pengfei Li was supported by National Natural Science Foundation of China [81904220].

Xiuhong Huang was supported by Science Research Cultivation Program of Stomatological Hospital, Southern Medical University [PY2022004].

Data availability statement

Data will be made available on request.

Declaration of interests statement

The authors declare no conflict of interest.

Additional information

Supplementary content related to this article has been published online at <https://doi.org/10.1016/j.heliyon.2022.e12101>.

Acknowledgements

The authors would like to acknowledge the Lingnan Medical Research Center for providing mechanical testing machine and the relevant hardware. The authors would also like to acknowledge Dr. Yueguang Fan for consultation.

References

Alomari, A.H., Wille, M.L., Langton, C.M., 2018. Bone volume fraction and structural parameters for estimation of mechanical stiffness and failure load of human cancellous bone samples; in-vitro comparison of ultrasound transit time spectroscopy and X-ray μ CT. *Bone* 107, 145–153.

Amini, M., Reisinger, A., Pahr, D.H., 2020. Influence of processing parameters on mechanical properties of a 3D-printed trabecular bone microstructure. *J. Biomed. Mater. Res. B Appl. Biomater.* 108, 38–47.

Awad, A., Fina, F., Goyanes, A., Gaisford, S., Basit, A.W., 2021. Advances in powder bed fusion 3D printing in drug delivery and healthcare. *Adv. Drug Deliv. Rev.* 174, 406–424.

Baptista, R., Guedes, M., 2021. Morphological and mechanical characterization of 3D printed PLA scaffolds with controlled porosity for trabecular bone tissue replacement. *Mater. Sci. Eng. C Mater. Biol. Appl.* 118, 1–17.

Barak, M.M., Black, M.A., 2018. A novel use of 3D printing model demonstrates the effects of deteriorated trabecular bone structure on bone stiffness and strength. *J. Mech. Behav. Biomed.* 78, 455–464.

Blake, G.M., Griffith, J.F., Yeung, D.K., Leung, P.C., Fogelman, I., 2009. Effect of increasing vertebral marrow fat content on BMD measurement, T-Score status and fracture risk prediction by DXA. *Bone* 44, 495–501.

Bouxsein, M.L., 2003. Bone quality: where do we go from here? *Osteoporos. Int.* 14, S118–S127.

Bouxsein, M.L., Boyd, S.K., Christiansen, B.A., Guldberg, R.E., Jepsen, K.J., Muller, R., 2010. Guidelines for assessment of bone microstructure in rodents using micro-computed tomography. *J. Bone Miner. Res.* 25, 1468–1486.

Bügra, B., Şeyma, D., 2022. Evaluation of mechanical behavior, bioactivity, and cytotoxicity of chitosan/akermanite-TiO₂ 3D-printed scaffolds for bone tissue applications. *Ceram. Int.* 48, 21419–21429.

Carter, D.R., Hayes, W.C., 1977. The compressive behavior of bone as a two-phase porous structure. *J. Bone Joint Surg. Am.* 59, 954–962.

Chen, W., Mao, M., Fang, J., Xie, Y., Rui, Y., 2022. Fracture risk assessment in diabetes mellitus. *Front. Endocrinol.* 13, 961761.

Davison, K.S., Kendler, D.L., Ammann, P., Bauer, D.C., Dempster, D.W., Dian, L., Hanley, D.A., Harris, S.T., McClung, M.R., Olszynski, W.P., et al., 2009. Assessing fracture risk and effects of osteoporosis drugs: bone mineral density and beyond. *Am. J. Med.* 122, 992–997.

Dobson, C.A., Sisiyas, G., Phillips, R., Fagan, M.J., Langton, C.M., 2006. Three dimensional stereolithography models of cancellous bone structures from μ CT data: testing and validation of finite element results. *Proc. Inst. Mech. Eng. H* 220, 481–484.

Doktor, T., Kumpová, I., Wroński, S., Śniechowski, M., Tarasiuk, J., Forte, G., Kytýř, D., 2018. Influence of printing and loading direction on mechanical response in 3D printed models of human trabecular bone. *Acta Polytechnica CTU Proc.* 18.

Grzeszczak, A., Lewin, S., Eriksson, O., Kreuger, J., Persson, C., 2021. The potential of stereolithography for 3D printing of synthetic trabecular bone structures. *Materials* 14.

Halgrin, J., Chaari, F., Markiewicz, E., 2012. On the effect of marrow in the mechanical behavior and crush response of trabecular bone. *J. Mech. Behav. Biomed. Mater.* 5, 231–237.

Hambli, R., 2013. Micro-CT finite element model and experimental validation of trabecular bone damage and fracture. *Bone* 56, 363–374.

Jin, Y., Zhang, T., Cheung, J.P.Y., Wong, T.M., Feng, X., Sun, T., Zu, H., Sze, K.Y., Lu, W.W., 2020. A novel mechanical parameter to quantify the microarchitecture effect on apparent modulus of trabecular bone: a computational analysis of ineffective bone mass. *Bone* 135, 115314.

Kabel, J., van Rietbergen, B., Dalstra, M., Odgaard, A., Huiskes, R., 1999. The role of an effective isotropic tissue modulus in the elastic properties of cancellous bone. *J. Biomech.* 32, 673–680.

Keaveny, T.M., Morgan, E.F., Niebur, G.L., Yeh, O.C., 2001. Biomechanics of trabecular bone. *Annu. Rev. Biomed. Eng.* 3, 307–333.

Keaveny, T.M., Clarke, B.L., Cosman, F., Orwoll, E.S., Siris, E.S., Khosla, S., Bouxsein, M.L., 2020. Biomechanical Computed Tomography analysis (BCT) for clinical assessment of osteoporosis. *Osteoporos. Int.* 31, 1025–1048.

Kim, Hokeun, Zhao, Yan, Zhao, L., 2016. Process-level modeling and simulation for HP's Multi Jet Fusion 3D printing technology. In: 2016 1st International Workshop on Cyber-Physical Production Systems (CPPS), pp. 1–4.

Kuhn, V., Ivanovic, N., Recheis, W., 2014a. High resolution 3D-printing of trabecular bone based on micro-CT data. *J. Orthop. Transl.* 4, 238.

Kuhn, V., Ivanovic, N., Recheis, W., 2014b. High resolution 3D-printing of trabecular bone based on microCT data. *J. Bone Miner. Res.* 29, S358. S358.

Langton, C.M., Whitehead, M.A., Langton, D.K., Langley, G., 1997. Development of a cancellous bone structural model by stereolithography for ultrasound characterisation of the calcaneus. *Med. Eng. Phys.* 19, 599–604.

Lewiecki, E.M., Wright, N.C., Curtis, J.R., Siris, E., Gagel, R.F., Saag, K.G., Singer, A.J., Steven, P.M., Adler, R.A., 2018. Hip fracture trends in the United States, 2002 to 2015. *Osteoporos. Int.* 29, 717–722.

Li, B.H., Aspden, R.M., 1997. Composition and mechanical properties of cancellous bone from the femoral head of patients with osteoporosis or osteoarthritis. *J. Bone Miner. Res.* 12, 641–651.

Linde, F., Norgaard, P., Hvid, I., Odgaard, A., Soballe, K., 1991. Mechanical properties of trabecular bone. Dependency on strain rate. *J. Biomech.* 24, 803–809.

Liu, X.S., Ardeshirpour, L., VanHouten, J.N., Shane, E., Wyslowski, J.J., 2012. Site-specific changes in bone microarchitecture, mineralization, and stiffness during lactation and after weaning in mice. *J. Bone Miner. Res.* 27, 865–875.

Liu, P., Liang, X., Li, Z., Zhu, X., Zhang, Z., Cai, L., 2019. Decoupled effects of bone mass, microarchitecture and tissue property on the mechanical deterioration of osteoporotic bones. *Compos. B Eng.* 177, 1–8.

Maquer, G., Musy, S.N., Wandel, J., Gross, T., Zysset, P.K., 2015. Bone volume fraction and fabric anisotropy are better determinants of trabecular bone stiffness than other morphological variables. *J. Bone Miner. Res.* 30, 1000–1008.

Maruyama, N., Shibata, Y., Wurihan Swain, M.V., Kataoka, Y., Takiguchi, Y., Yamada, A., Maki, K., Miyazaki, T., 2014. Strain-rate stiffening of cortical bone: observations and implications from nanoindentation experiments. *Nanoscale* 6, 14863–14871.

Matter, H.P., Garrel, T.V., Bilderbeek, U., Mittelmeier, W., 2001. Biomechanical examinations of cancellous bone concerning the influence of duration and temperature of cryopreservation. *J. Biomed. Mater. Res.* 55, 40–44.

McNamara, L.M., 2010. Perspective on post-menopausal osteoporosis: establishing an interdisciplinary understanding of the sequence of events from the molecular level to whole bone fractures. *J. R. Soc. Interface* 7, 353–372.

Mohammad Reza, K., Ali, Z., Matt, J., Tamara, R., 2020. Structural performance of 3D-printed composites under various loads and environmental conditions. *Polym. Test.* 91, 106770.

Morgan, E.F., Bayraktar, H.H., Keaveny, T.M., 2003. Trabecular bone modulus-density relationships depend on anatomic site. *J. Biomech.* 36, 897–904.

Morgan, E.F., Unnikrisnan, G.U., Hussein, A.I., 2018. Bone mechanical properties in healthy and diseased states. *Annu. Rev. Biomed. Eng.* 20, 119–143.

NCDPoO, P., 2001. Osteoporosis prevention, diagnosis, and therapy. *JAMA* 285, 785–795.

Ni, M., Wong, D.W., Mei, J., Niu, W., Zhang, M., 2016. Biomechanical comparison of locking plate and crossing metallic and absorbable screws fixations for intra-articular calcaneal fractures. *Sci. China Life Sci.* 59, 958–964.

- Nofar, M., Salehiyan, R., Ray, S.S., 2019. Rheology of poly (lactic acid)-based systems. *Polym. Rev.* 59, 465–509.
- Ouyang, J., Yang, G.T., Wu, W.Z., Zhu, Q.A., Zhong, S.Z., 1997. Biomechanical characteristics of human trabecular bone. *Clin. Biomech.* 12, 522–524.
- Pilcher, A., Wang, X., Kaltz, Z., Garrison, J.G., Niebur, G.L., Mason, J., Song, B., Cheng, M., Chen, W., 2010. High strain rate testing of bovine trabecular bone. *J. Biomech. Eng.* 132, 081012.
- Promnil, S., Ruksakulpiwat, C., Numpaisal, P.O., Ruksakulpiwat, Y., 2022. Electrospun poly(lactic acid) and silk fibroin based nanofibrous scaffold for meniscus tissue engineering. *Polymers* 14.
- Reid, I.R., 2021. Revisiting osteoporosis guidelines. *Lancet Diabetes Endocrinol.* 9, 805–806.
- Senatov, F.S., Niaza, K.V., Stepashkin, A.A., Kaloshkin, S.D., 2016. Low-cycle fatigue behavior of 3d-printed PLA-based porous scaffolds. *Compos. B Eng.* 97, 193–200.
- Silva, M.J., Keaveny, T.M., Hayes, W.C., 1998. Computed tomography-based finite element analysis predicts failure loads and fracture patterns for vertebral sections. *J. Orthop. Res.* 16, 300–308.
- Singh, A.P., Pervaiz, S., 2021. Current Status and Prospects of Multi-Jet Fusion (MJF) Based 3D Printing Technology. Paper Presented at: ASME 2021 International Mechanical Engineering Congress and Exposition.
- Tassani, S., Ohman, C., Baruffaldi, F., Baleani, M., Viceconti, M., 2011. Volume to density relation in adult human bone tissue. *J. Biomech.* 44, 103–108.
- Tellis, B.C., Szivek, J.A., Bliss, C.L., Margolis, D.S., Vaidyanathan, R.K., Calvert, P., 2008. Trabecular scaffolds created using micro CT guided fused deposition modeling. *Mat. Sci. Eng. C-Bio S.* 28, 171–178.
- Tiefenboeck, T.M., Payr, S., Bajenov, O., Koch, T., Komjati, M., Sarahrudi, K., 2019. Effect of two (short-term) storage methods on load to failure testing of murine bone tissue. *Sci. Rep.* 9, 5961.
- Tiefenboeck, T.M., Payr, S., Bajenov, O., Dangl, T., Koch, T., Komjati, M., Sarahrudi, K., 2020. Different storage times and their effect on the bending load to failure testing of murine bone tissue. *Sci. Rep. Uk* 10.
- Uniyal, P., Sihota, P., Kumar, N., 2022. Effect of organic matrix alteration on strain rate dependent mechanical behaviour of cortical bone. *J. Mech. Behav. Biomed. Mater.* 125, 104910.
- Uppuganti, S., Ketsiri, T., Zhang, Y., Does, M.D., Nyman, J.S., 2022. HR-pQCT parameters of the distal radius correlate with the bending strength of the radial diaphysis. *Bone* 161, 116429.
- Wood, Z., Lynn, L., Nguyen, J.T., Black, M.A., Patel, M., Barak, M.M., 2019. Are we crying Wolff? 3D printed replicas of trabecular bone structure demonstrate higher stiffness and strength during off-axis loading. *Bone* 127, 635–645.
- Wu, D., Spanou, A., Diez-Escudero, A., Persson, C., 2020. 3D-printed PLA/HA composite structures as synthetic trabecular bone: a feasibility study using fused deposition modeling. *J. Mech. Behav. Biomed. Mater.* 103, 103608.
- Yoon, Y.J., Moon, S.K., Hwang, J., 2014. 3D printing as an efficient way for comparative study of biomimetic structures - trabecular bone and honeycomb. *J. Mech. Sci. Technol.* 28, 4635–4640.
- Zhang, J., Delzell, E., Zhao, H., Laster, A.J., Saag, K.G., Kilgore, M.L., Morrisey, M.A., Wright, N.C., Yun, H., Curtis, J.R., 2012. Central DXA utilization shifts from office-based to hospital-based settings among medicare beneficiaries in the wake of reimbursement changes. *J. Bone Miner. Res.* 27, 858–864.
- Zhang, Z.M., Li, Z.C., Jiang, L.S., Jiang, S.D., Dai, L.Y., 2010. Micro-CT and mechanical evaluation of subchondral trabecular bone structure between postmenopausal women with osteoarthritis and osteoporosis. *Osteoporos. Int.* 21, 1383–1390.
- Zheng, L., Dai, Y., Zheng, Y., He, X., Wu, M., Zheng, D., Li, C., Fan, Y., Lin, Z., 2022. Medial tibial plateau sustaining higher physiological stress than the lateral plateau: based on 3D printing and finite element method. *Biomed. Eng. Online* 21.
- Zhou, B., Wang, J., Yu, Y.E., Zhang, Z., Nawathe, S., Nishiyama, K.K., Rosete, F.R., Keaveny, T.M., Shane, E., Guo, X.E., 2016. High-resolution peripheral quantitative computed tomography (HR-pQCT) can assess microstructural and biomechanical properties of both human distal radius and tibia: Ex vivo computational and experimental validations. *Bone* 86, 58–67.